

Supplementary Material

Pocket Formation and Behavior in Turbulent Premixed Flames

Ankit Tyagi¹, Isaac Boxx², Stephen Peluso¹, Jacqueline O'Connor¹
¹*Mechanical Engineering, Pennsylvania State University, University Park, PA, USA*
²*German Aerospace Center (DLR), Stuttgart, Germany*

A. Flame surface density images

Figure S1-Figure S6 show flame surface density images for cases A-Single, C-Single, E-Single, A-Dual, C-Dual, and E-Dual flame cases. In each of these figures, sub-figure (a) shows the total flame surface density, sub-figure (b) shows the flame surface density contributions from all flame pockets, sub-figure (c) shows the flame surface density contributions from reactant pockets, and sub-figure (d) shows the flame surface density contributions from product pockets.

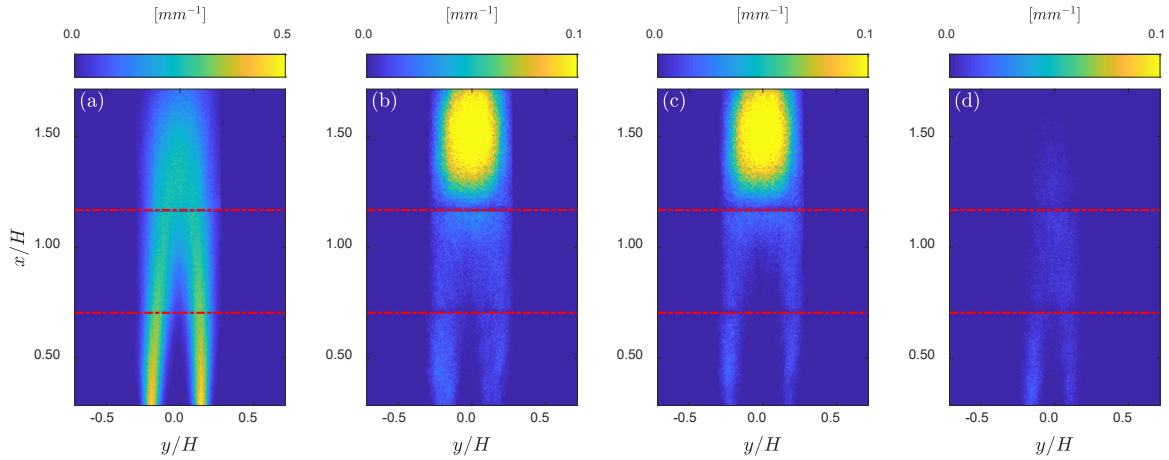


Figure S1: Flame surface density contributions for flame A-Single: (a) total, (b) all pocket contributions, (c) reactant pocket contributions, and (d) product pocket contributions

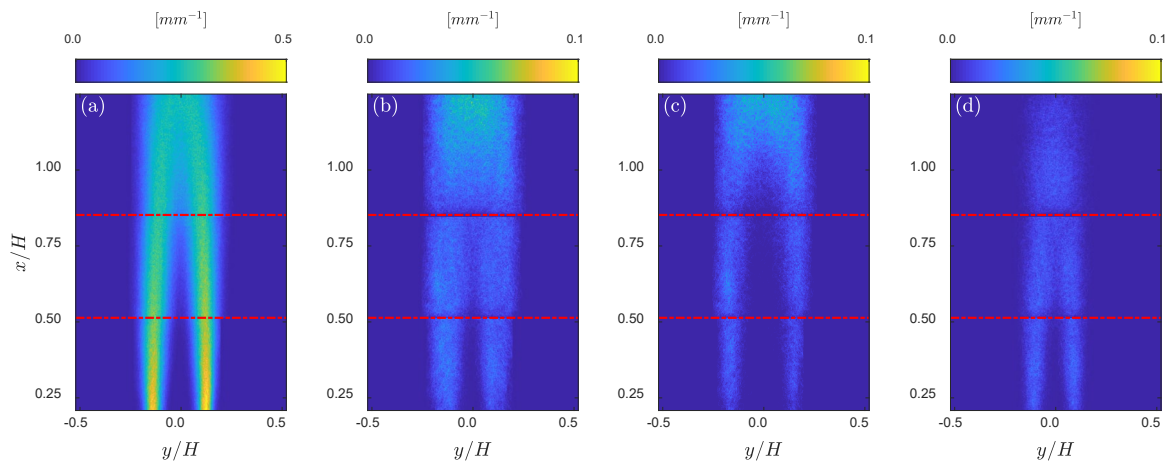


Figure S2: Flame surface density contributions for flame C-Single: (a) total, (b) all pocket contributions, (c) reactant pocket contributions, and (d) product pocket contributions

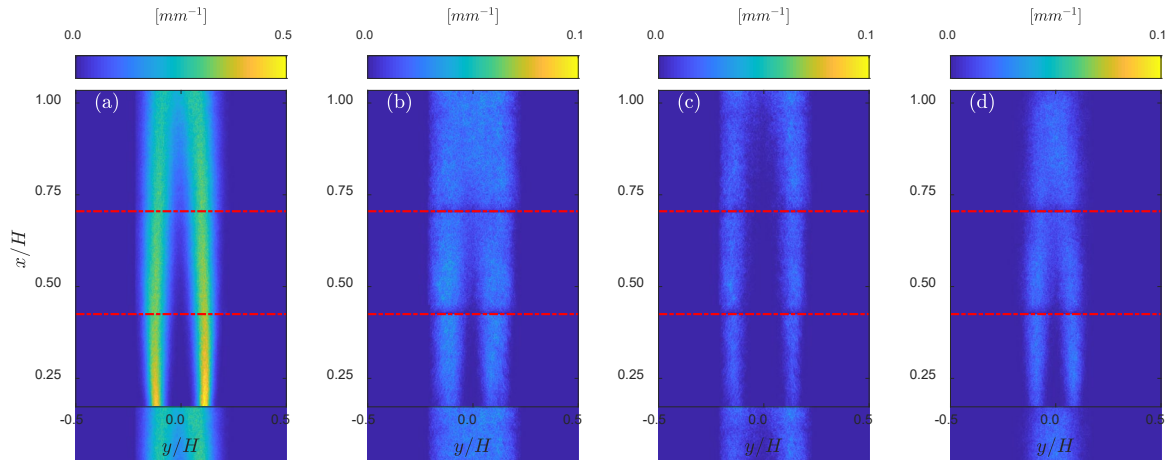


Figure S3: Flame surface density contributions for flame E-Single: (a) total, (b) all pocket contributions, (c) reactant pocket contributions, and (d) product pocket contributions

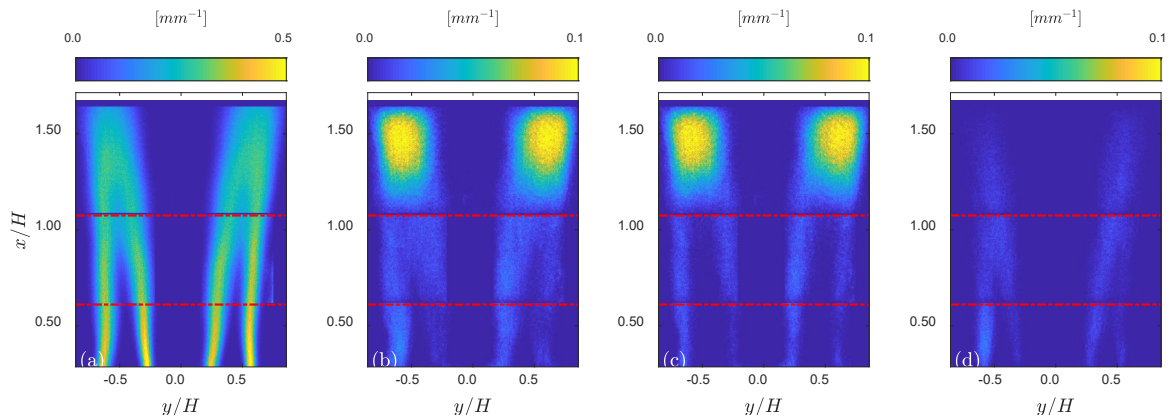


Figure S4: Flame surface density contributions for flame A-Dual: (a) total, (b) all pocket contributions, (c) reactant pocket contributions, and (d) product pocket contributions

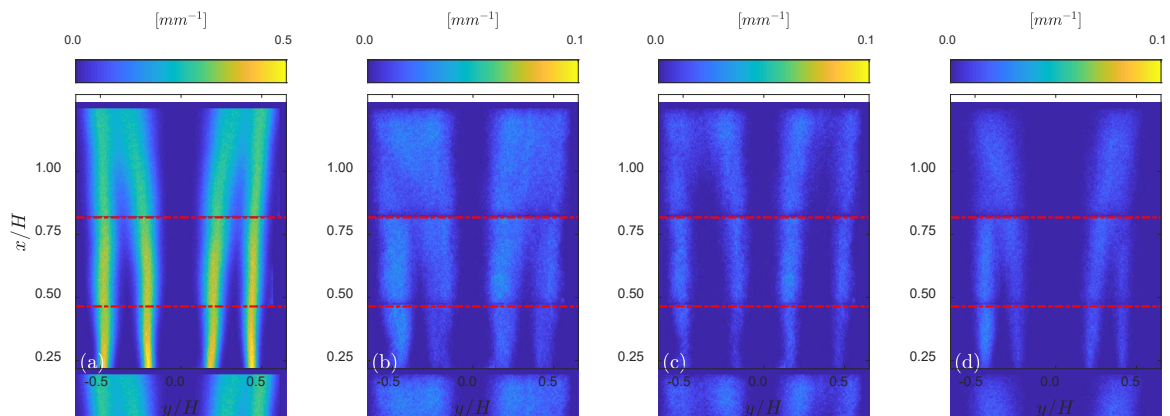


Figure S5: Flame surface density contributions for flame C-Dual: (a) total, (b) all pocket contributions, (c) reactant pocket contributions, and (d) product pocket contributions

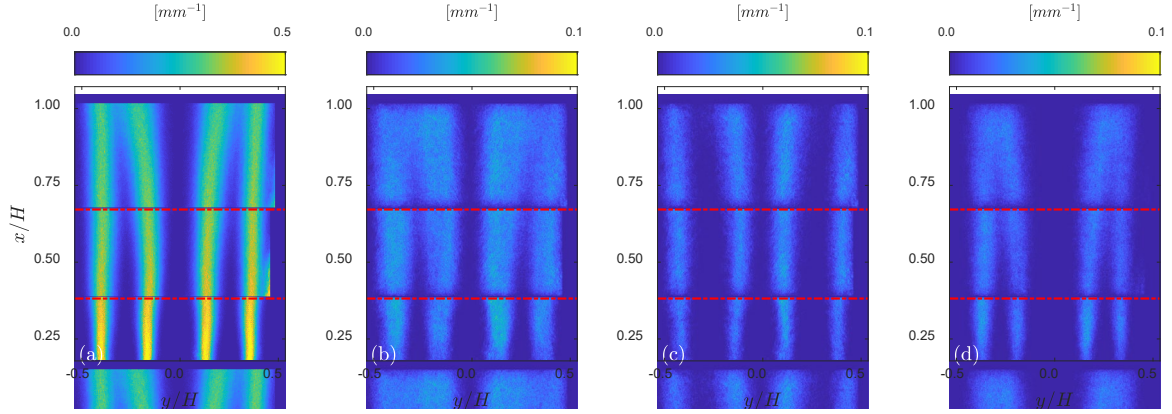


Figure S6: Flame surface density contributions for flame E-Dual: (a) total, (b) all pocket contributions, (c) reactant pocket contributions, and (d) product pocket contributions

B. Effect of pockets on consumption speed

The impact of reactant and product pockets on global consumption speeds is also considered; time-averaged progress variable contours (\bar{c}) are obtained at a value of 0.2 for each case with and without flames pockets to calculate a global consumption speed, given in Equation (1):

$$S_{T,GC\bar{c}} = \dot{m}_R / \rho_R A_{\bar{c}=0.2} \quad (1)$$

This definition of global consumption speed has been commonly used in literature^{1, 2} and we choose to use a progress variable contour based on $\bar{c}=0.2$ because capturing a closed contour at $\bar{c}=0.5$ is not possible in FOV III for cases C and E. Results of global consumption speed calculations with and without flame pockets are presented in Table S1. For increasing Reynolds

¹ J.F. Driscoll, Turbulent premixed combustion: Flamelet structure and its effect on turbulent burning velocities, Progress in Energy and Combustion Science 34 (2008) 91-134.

² S.A. Filatyev, J.F. Driscoll, C.D. Carter, J.M. Donbar, Measured properties of turbulent premixed flames for model assessment, including burning velocities, stretch rates, and surface densities, Combustion and Flame 141 (2005) 1-21.

number (cases A - E), the value of $S_{T,GC\bar{c}}$ increases as a result of increased turbulence level. Comparisons of $S_{T,GC\bar{c}}$ values with the inclusion and exclusion of reactant and product pockets shows that flame pockets do not significantly impact the global consumption rates of the reactants.

Table S1: Comparison of global consumption speeds ($S_{T,GC\bar{c}}$) with and without flame pockets

Case	Total	Without pockets	$S_{T,GC\bar{c}}$ [m/s]	
			Without reactant pockets	Without product pockets
A-Single	2.7	2.7	2.7	2.7
A-Dual	2.3	2.3	2.3	2.3
C-Single	3.2	3.2	3.2	3.2
C-Dual	2.8	2.7	2.8	2.7
E-Single	3.6	3.5	3.6	3.5
E-Dual	3.1	3.0	3.1	3.0

C. Lifetime of flame pockets

Figure S7-Figure S10 show the scatter plots of pocket lifetimes vs. mean pocket radii for reactant and product pockets in single- and dual-flames cases presented in this study. In these figures, it is shown that the pocket lifetimes are usually lower than 0.5 milli-seconds, which corresponds to 5 frames for a 10 kHz data acquisition frame rate. This indicates that most pockets exist for a short time and resolving this lifetime using the current sampling rate (10 kHz) is sufficient for most of the pockets.

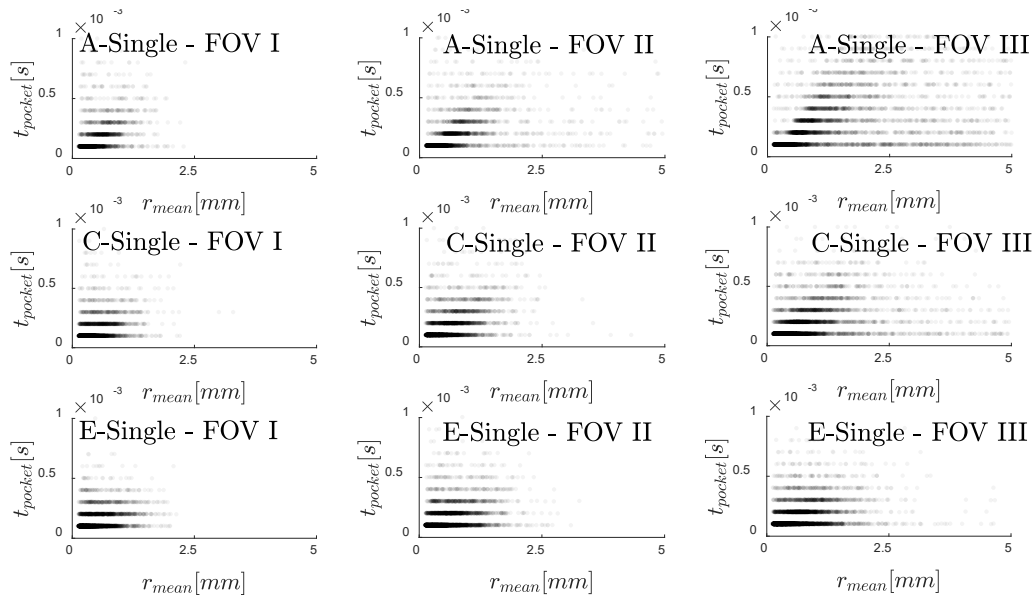


Figure S7: Scatter plots of mean pocket radii and pocket lifetimes for reactant pockets in single-flames

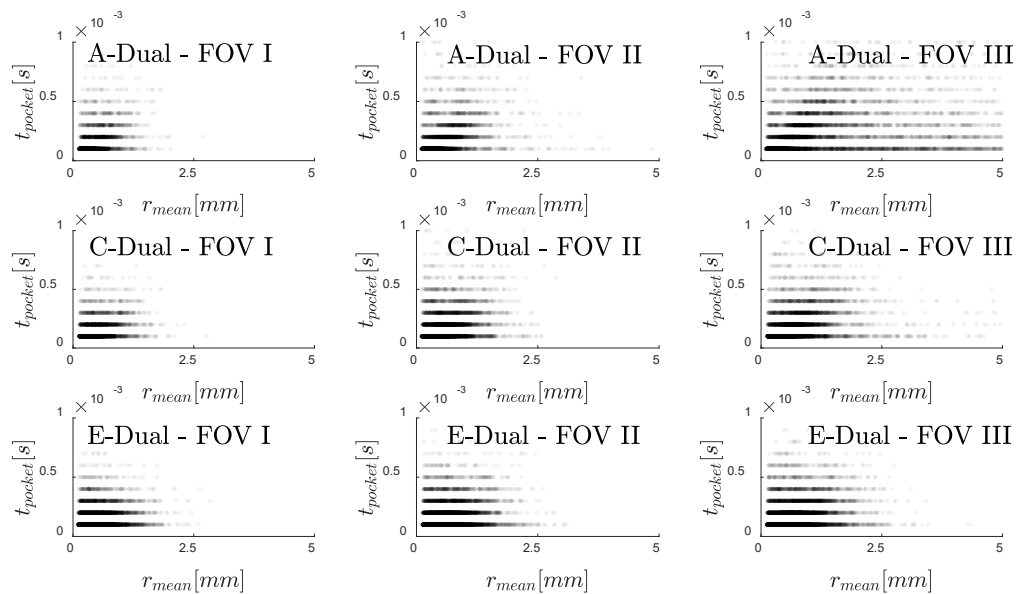


Figure S8: Scatter plots of mean pocket radii and pocket lifetimes for reactant pockets in dual-flames

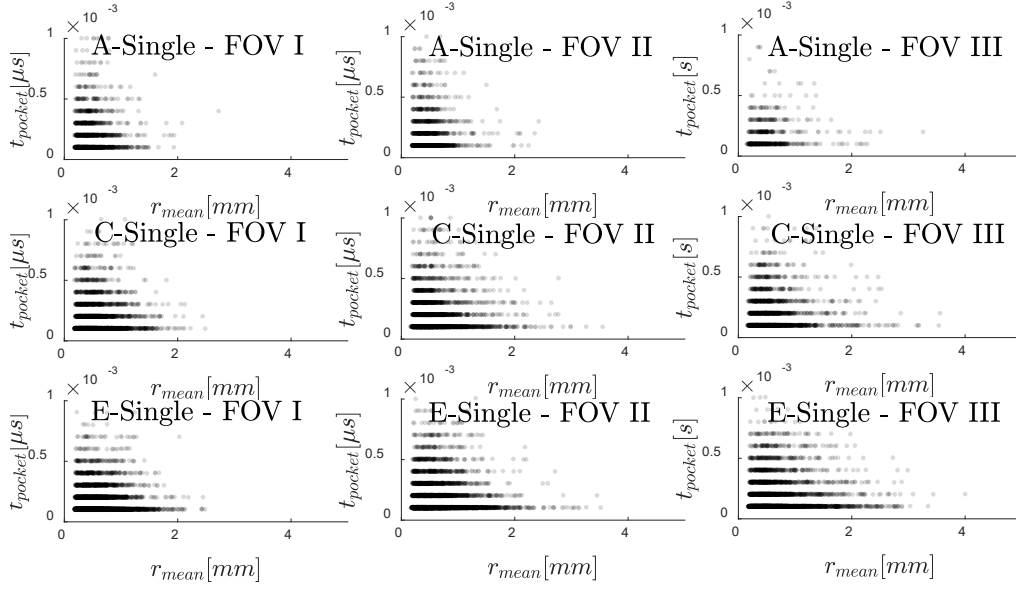


Figure S9: Scatter plots of mean pocket radii and pocket lifetimes for product pockets in single-flames

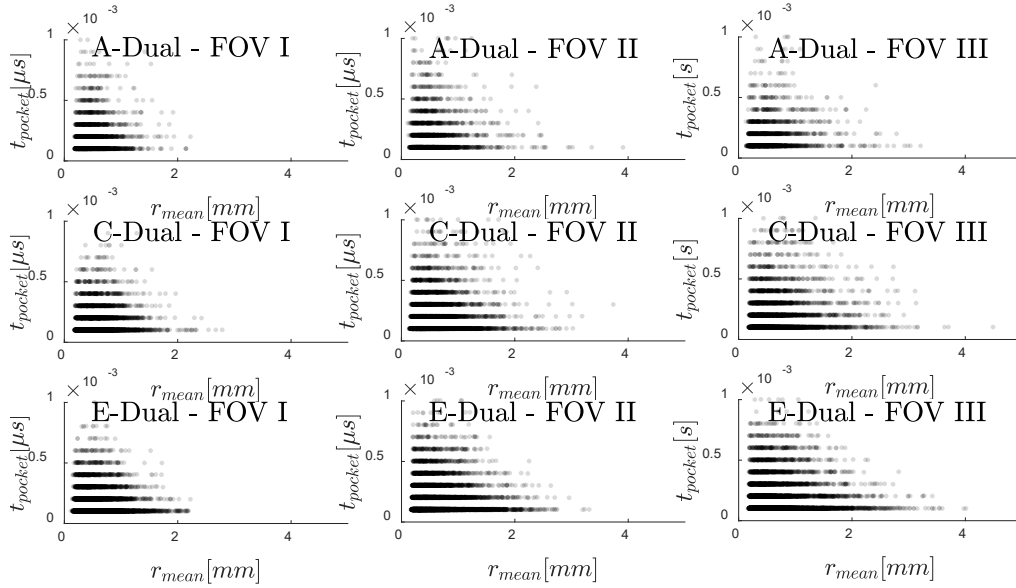


Figure S10: Scatter plots of mean pocket radii and pocket lifetimes for product pockets in dual-flames

D. Turbulence intensities along jet centerlines

Figure S11 shows the turbulence intensities along the jet centerlines for dual-flames cases A, C, and E. Sub-figure (a) shows the total turbulence intensity and sub-figure (b) shows the turbulence intensities along the x , y , and z directions. Figure S12 shows the turbulence intensities along different contour levels for Case E-Dual.

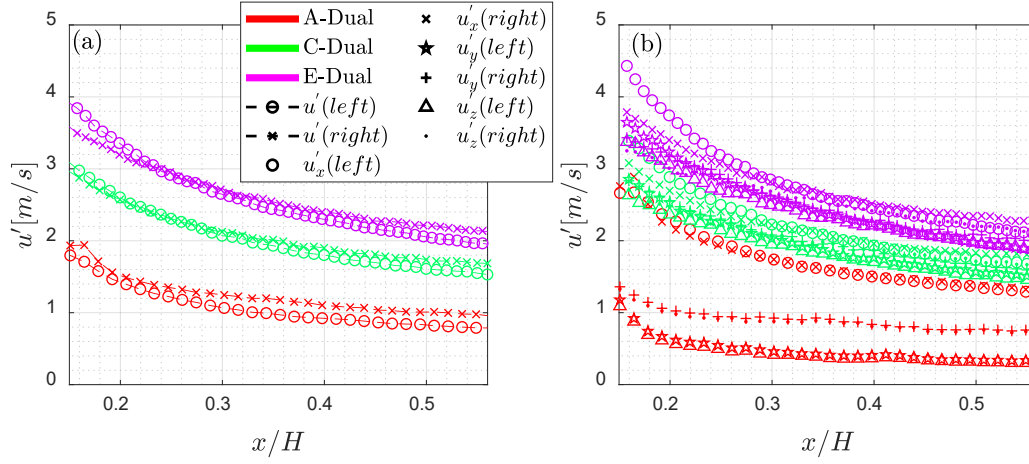


Figure S11: (a) Total turbulence intensities (u') and (b) components of turbulence intensities (u'_x , u'_y , and u'_z) along jet centerlines for dual-flames cases A, C, and E.

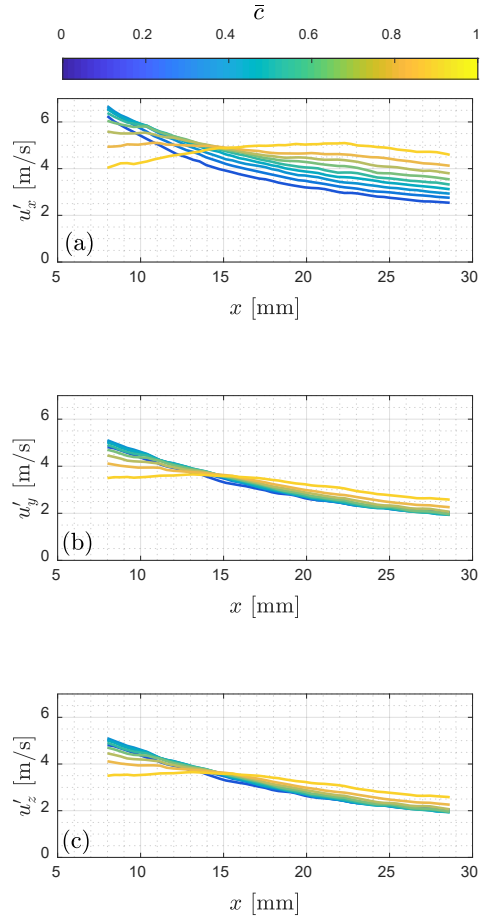


Figure S12: Turbulence intensities along different time-averaged progress variable contours for E-Dual case: (a) u'_x , (b) u'_y , and (c) u'_z